iScience

CellPress
OPEN ACCESS

Article

Carbohydrate metabolism is a determinant for the host specificity of baculovirus infections

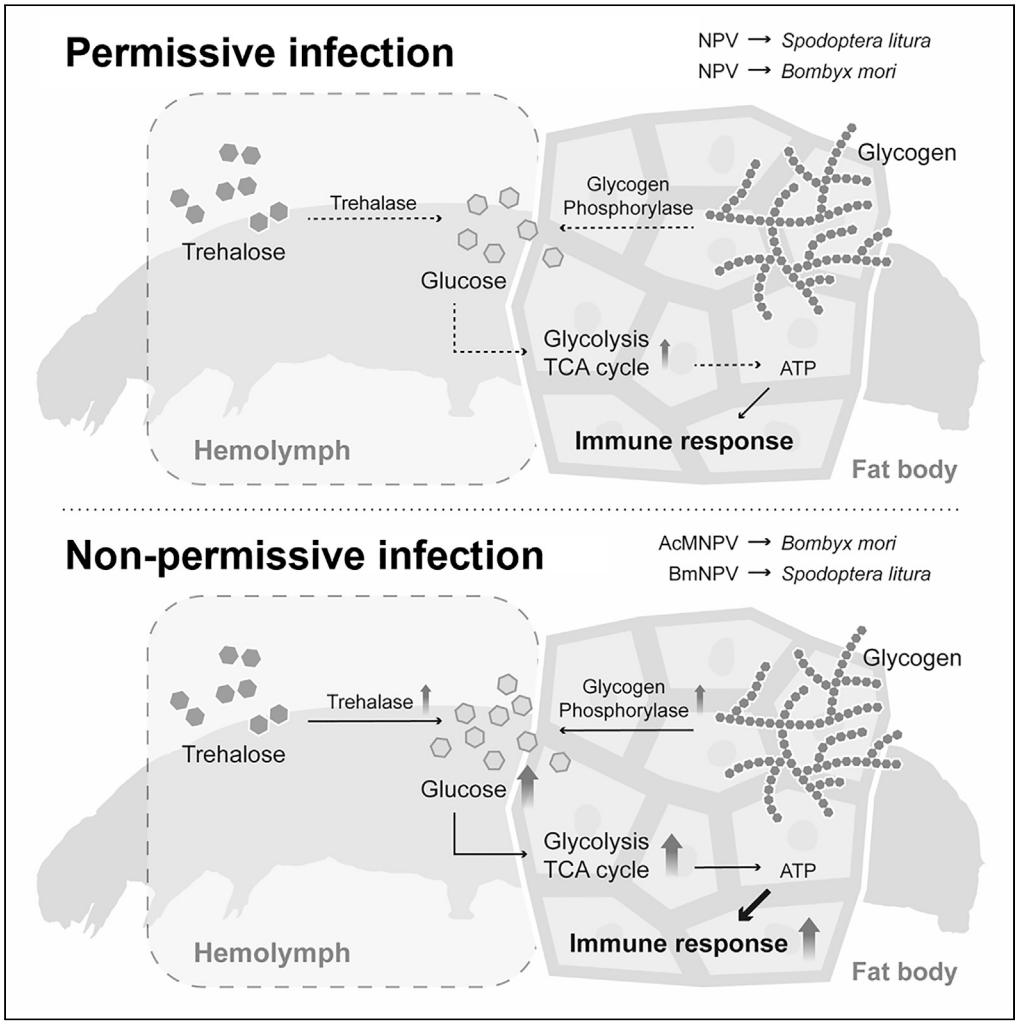

Chih-Hsuan Tsai, Yi-Chi Chuang, Yun-Heng Lu, Chia-Yang Lin, Cheng-Kang Tang, Sung-Chan Wei, Yueh-Lung Wu

runwu@ntu.edu.tw

Highlights

Nonpermissive infections by AcMNPV and BmNPV alter host carbohydrate metabolism

Increased carbohydrate metabolism produces energy to launch immune responses

Immune responses including antimicrobial peptide production inhibit virus infection

Host metabolic alterations affect the determination of virus's host specificity

Tsai et al., iScience 25, 103648
January 21, 2022
https://doi.org/10.1016/j.isci.2021.103648

iScience

CellPress
OPEN ACCESS

Article

Carbohydrate metabolism is a determinant for the host specificity of baculovirus infections

Chih-Hsuan Tsai,[1,2] Yi-Chi Chuang,[1,2] Yun-Heng Lu,[1] Chia-Yang Lin,[1] Cheng-Kang Tang,[1] Sung-Chan Wei,[1] and Yueh-Lung Wu[1,3,*]

SUMMARY

Baculoviruses Autographa californica multicapsid nucleopolyhedrovirus (AcMNPV) and Bombyx mori nucleopolyhedrovirus (BmNPV) have highly similar genome sequences but exhibit no overlap in their host range. After baculovirus infects nonpermissive larvae (e.g., AcMNPV infecting *B. mori* or BmNPV infecting *Spodoptera litura*), we found that stored carbohydrates, including hemolymph trehalose and fat body glycogen, are rapidly transformed into glucose; enzymes involved in glycolysis and the TCA cycle are upregulated and produce more ATP; adenosine signaling that regulates glycolytic activity is also increased. Subsequently, phagocytosis in cellular immunity and the expression of genes involved in humoral immunity increase significantly. Moreover, inhibiting glycolysis and the expression of goverins in nonpermissive hosts increased baculovirus infectivity, indicating that the stimulated energy production is designed to support the immune response against infection. Our study highlights that alteration of the host's carbohydrate metabolism is an important factor determining the host specificity of baculoviruses, in addition to viral factors.

INTRODUCTION

Baculoviruses are large, double-stranded DNA viruses that infect insects and many other arthropods (Groner, 1986). Autographa californica multicapsid nucleopolyhedrovirus (AcMNPV) and Bombyx mori nucleopolyhedrovirus (BmNPV), are the two most thoroughly studied baculoviruses and both have been extensively applied in the expression of eukaryotic recombinant proteins (Gomi et al., 1999; Vail et al., 1971). Although the amino acid sequence identity of open reading frames (ORF) between AcMNPV and BmNPV is as high as 93% (Gomi et al., 1999), the two viruses exhibit highly distinct infection profiles. AcMNPV is capable of infecting over 39 lepidopteran insect larvae, e.g., *Spodoptera frugiperda* and *Trichoplusia ni*, but not the silkworm *B. mori*. In contrast, BmNPV specifically replicates in the cell lines and larva of *B. mori*, but not in those of other lepidopteran species (Kondo and Maeda, 1991; Sakurai et al., 1998). This makes AcMNPV and BmNPV a good pair target for studying host specificity. Previous studies have identified amino acid mutations in DNA helicase P143 (Croizier et al., 1994) and the substitution of envelope glycoprotein GP64 (Katou et al., 2006) that enable AcMNPV or BmNPV to infect nonpermissive cell lines. However, little research has been undertaken on how the host responds to these infections and whether this determines if an infection is permissive or nonpermissive.

Pathogen invasion triggers an immune response in the host. In *Spodoptera litura*, an increased immune response was shown to inhibit infection by a polydnavirus (Chang et al., 2020), indicating that the host immune response may play a determinative role in viral infection. In insects, immune responses include both cellular and humoral immunity (Blandin and Levashina, 2004; Crozatier et al., 2004; Gillespie et al., 1997; Strand and Pech, 1995). In cellular immunity, hemocytes phagocytose or encapsulate the invading pathogens, and induce melanization to destroy the pathogens. Humoral immunity, on the other hand, involves the production of antimicrobial peptides (AMPs) to respond to microbial invasions (Morishima et al., 1995). When an insect host is invaded by microbes, the humoral immune pathways, Toll, IMD, and JAK/STAT, activate AMP production in the hemocytes and fat body cells (Ferrandon et al., 1998; Tzou et al., 2000). For instance, gloverin, a lepidopteran-specific AMP, is involved in the defense against Gram-negative bacteria, and Gloverin-4, one of the four gloverins identified in *B. mori*, has been found to confer viral resistance to the larva (Bao et al., 2009). In *T. ni*, gloverins have also been shown to inhibit AcMNPV replication, probably through disruption of the viral envelope (Moreno-Habel et al., 2012).

[1]Department of Entomology, National Taiwan University, 27 Lane 113, Roosevelt Road Sec. 4, Taipei 106, Taiwan

[2]These authors contributed equally

[3]Lead contact

*Correspondence: runwu@ntu.edu.tw

https://doi.org/10.1016/j.isci.2021.103648

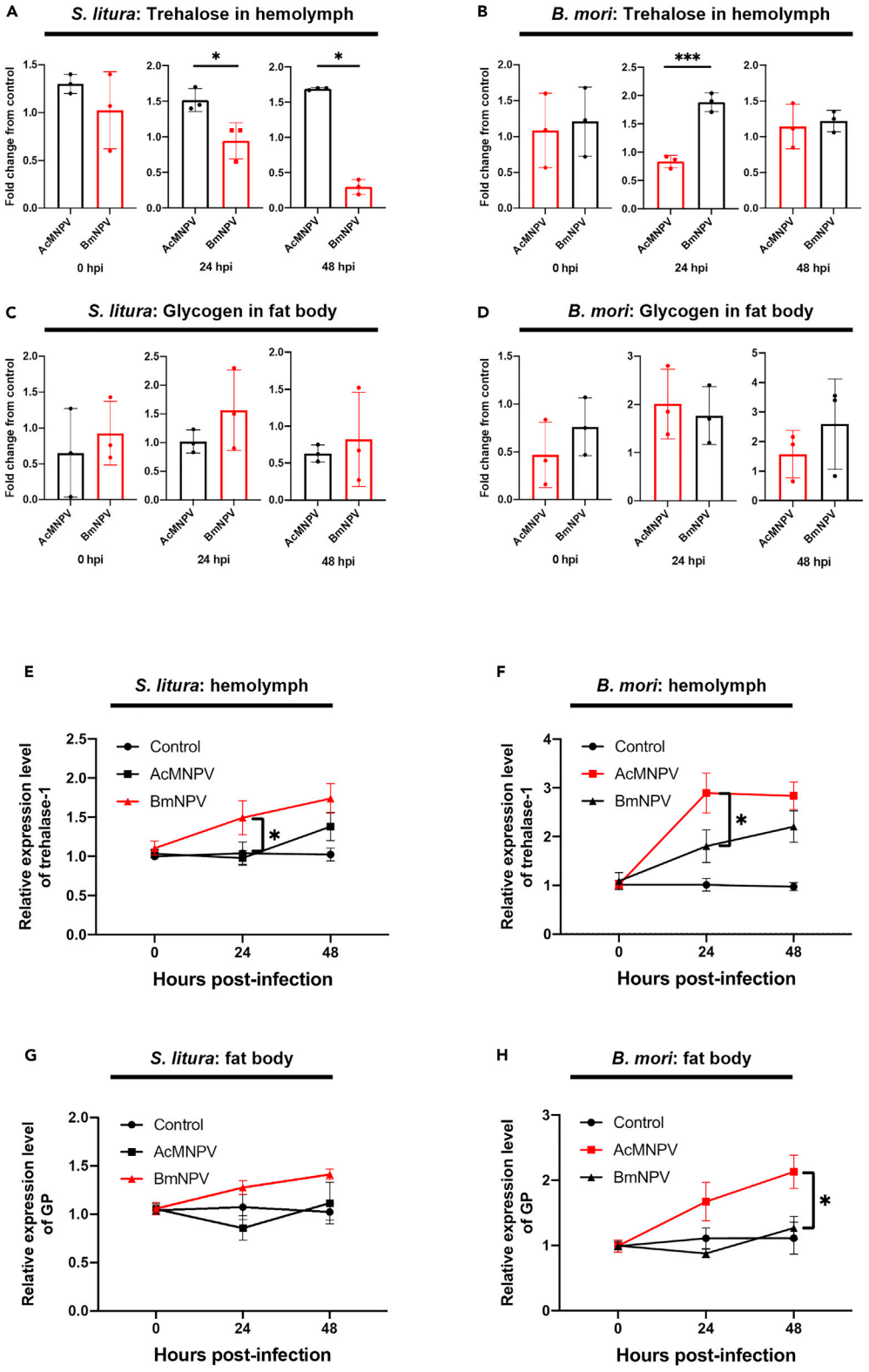
A
S. litura: Trehalose in hemolymph
B
B. mori: Trehalose in hemolymph
C
S. litura: Glycogen in fat body
D
B. mori: Glycogen in fat body
Fold change from control
AcMNPV
BmNPV
0 hpi
24 hpi
48 hpi
E
S. litura: hemolymph
F
B. mori: hemolymph
G
S. litura: fat body
H
B. mori: fat body
Control
AcMNPV
BmNPV
Relative expression level of trehalase-1
Relative expression level of GP
Hours post-infection

Figure 1. The effects of permissive and nonpermissive infection on the metabolism of trehalose and glycogen in the hemolymph and fat body of *S. litura* and *B. mori* larvae

(A and B) *S. litura* (A) and *B. mori* (B) (n = 3) were infected with AcMNPV and BmNPV, and the trehalose concentration in the hemolymph was determined at 0, 24, and 48 hpi.

(C and D) The fat body was also isolated from *S. litura* (C) and *B. mori* (D) larvae after virus infection, and the glycogen concentration determined at 0, 24, and 48 hpi. Data are expressed as mean ± standard deviation (SD) of the fold changes relative to the uninfected control.

(E–H) Expression levels of trehalase-1 in the hemolymph of *S. litura* (E) and *B. mori* (F), and of glycogen phosphorylase in the fat body of *S. litura* (G) and *B. mori* (H) were determined at 0, 24, and 48 hpi for both AcMNPV and BmNPV infection. Gene expression levels were quantified using Quantitative reverse transcription PCR (RT-qPCR). Data for each condition (n = 3) are normalized to the expression of the *18S* gene and expressed as mean ± SD of the relative ratio to the uninfected control. Student's *t*-test was used to determine the statistically significant differences (*p <0.05; ***p <0.005). Black and red bars/lines indicate permissive and nonpermissive infection conditions, respectively.

For a rapid and effective immune response, a large amount of energy is required (Dolezal et al., 2019). In insects, energy is derived from carbohydrate sources such as glycogen stored in the fat body and trehalose in the hemolymph. These two stored sugars are enzymatically converted into glucose, which is then used in the production of high-energy ATP through glycolysis and the tricarboxylic acid (TCA) cycle (Becker et al., 1996; Steele, 1982). A previous transcriptomic analysis in mosquitos revealed that genes involved in the respiratory chain were upregulated in hemocytes upon bacterial infection (Bartholomay et al., 2004). Furthermore, when *Drosophila* larvae were infected by parasitoid wasps or bacteria, significant amounts of nutrients, especially glucose, were distributed to the hemolymph to fuel immune cell development (Bajgar and Dolezal, 2018; Bajgar et al., 2015). These nutrients are temporarily diverted from those needed for host development (DiAngelo et al., 2009; Yang and Hultmark, 2017). This metabolic switch is clearly essential for antiviral responses, because starvation or blocking the signal transduction for metabolic reprogramming has been found to decrease the immune response against pathogens (Bajgar and Dolezal, 2018; Bajgar et al., 2015; Yang and Hultmark, 2017).

Because metabolic switching is of great significance to antiviral responses, we postulated that (a) the host's metabolic reactions may differ depending on whether an infection was permissive or non-permissive, and (b) it is the successful redirection of energy that results in virus replication being inhibited for a nonpermissive infection. As such, we investigated the carbohydrate metabolism and immune responses in the larvae of *S. litura* and *B. mori* after permissive (*S. litura*: AcMNPV; *B. mori*: BmNPV) and nonpermissive (*S. litura*: BmNPV; *B. mori*: AcMNPV) infections. We determined the level of stored carbohydrates, glucose, and ATP, and the expression of enzymes in metabolic pathways. Both cellular and humoral immune responses were also examined in the larvae, via phagocytosis and gloverin production, respectively. We observed that nonpermissive infections increased carbohydrate metabolism and elicited stronger immune responses than permissive infections. Furthermore, we tested whether inhibiting glycolysis or decreasing gloverin production could alter the host specificity of the two viruses. Our results suggest that virus infections in nonpermissive hosts are inhibited by immune responses driven by the redirected energy.

RESULTS

Nonpermissive infection increases the metabolism of stored sugars in the larvae

To determine changes in carbohydrate levels during permissive and nonpermissive infection, *S. litura* and *B. mori* larvae were infected with baculoviruses AcMNPV and BmNPV. After permissive infections (i.e., infection of *S. litura* larvae with AcMNPV and *B. mori* larvae with BmNPV) for two days, approximately 1×10^7 plaque-forming units (PFU)/mL of the virus could be detected in the body fluid of both larvae. In contrast, for the nonpermissive infections only 1×10^3 PFU/mL of BmNPV and 1×10^2 PFU/mL of AcMNPV were detected in the body fluid of *S. litura* and *B. mori* larvae, respectively.

Levels of the two sugar storage molecules, trehalose and glycogen, were measured in the hemolymph and fat body of the infected larvae. The results showed that the trehalose levels in the hemolymph of nonpermissive larvae (BmNPV-infected *S. litura* and AcMNPV-infected *B. mori*) were significantly lower than those of permissive larvae (AcMNPV-infected *S. litura* and BmNPV-infected *B. mori*) at 24 h postinfection (hpi) (Figures 1A and 1B). However, in the fat body, no significant difference in trehalose content was found between permissive and nonpermissive infections (Figures S1A and S1B). For glycogen, the main sugar stored in the fat body, we found that the level did not change significantly in the fat body for any of the test groups (Figures 1C and 1D).

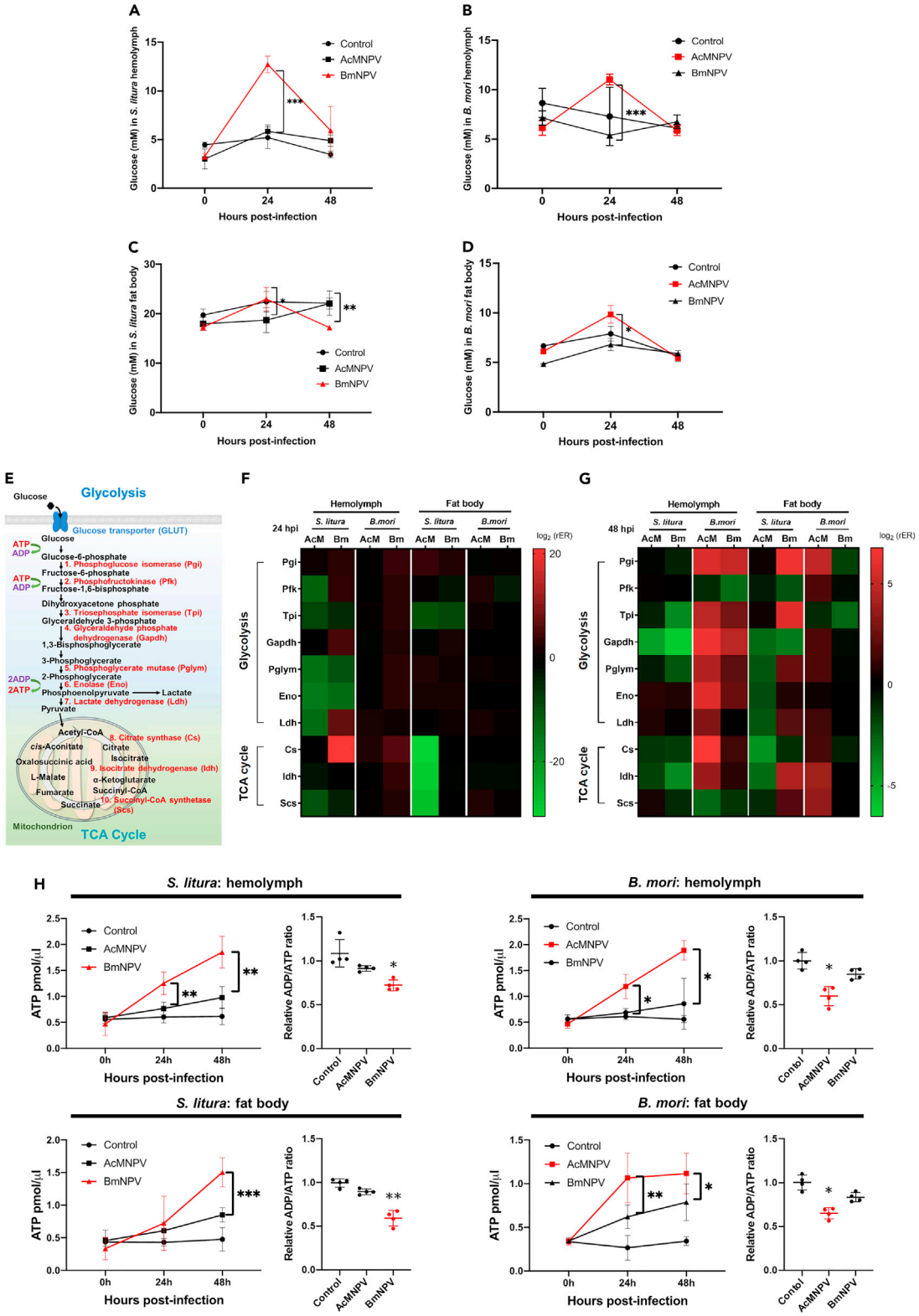
A
Glucose (mM) in S. litura hemolymph
Hours post-infection
Control
AcMNPV
BmNPV
***
B
Glucose (mM) in B. mori hemolymph
Hours post-infection
Control
AcMNPV
BmNPV
***
C
Glucose (mM) in S. litura fat body
Hours post-infection
Control
AcMNPV
BmNPV
*
**
D
Glucose (mM) in B. mori fat body
Hours post-infection
Control
AcMNPV
BmNPV
*
E
Glycolysis
Glucose
Glucose transporter (GLUT)
Glucose
ATP
ADP
Glucose-6-phosphate
1. Phosphoglucose isomerase (Pgi)
Fructose-6-phosphate
ATP
ADP
2. Phosphofructokinase (Pfk)
Fructose-1,6-bisphosphate
Dihydroxyacetone phosphate
3. Triosephosphate isomerase (Tpi)
Glyceraldehyde 3-phosphate
4. Glyceraldehyde phosphate dehydrogenase (Gapdh)
1,3-Bisphosphoglycerate
3-Phosphoglycerate
5. Phosphoglycerate mutase (Pglym)
2-Phosphoglycerate
2ADP
2ATP
6. Enolase (Eno)
Phosphoenolpyruvate
Lactate
7. Lactate dehydrogenase (Ldh)
Pyruvate
Acetyl-CoA
8. Citrate synthase (Cs)
cis-Aconitate
Citrate
Isocitrate
Oxalosuccinic acid
9. Isocitrate dehydrogenase (Idh)
L-Malate
α-Ketoglutarate
Fumarate
Succinyl-CoA
10. Succinyl-CoA synthetase (Scs)
Succinate
Mitochondrion
TCA Cycle
F
24 hpi
Hemolymph
Fat body
S. litura
B.mori
AcM
Bm
log2 (rER)
Glycolysis
TCA cycle
Pgi
Pfk
Tpi
Gapdh
Pglym
Eno
Ldh
Cs
Idh
Scs
G
48 hpi
Hemolymph
Fat body
S. litura
B.mori
AcM
Bm
log2 (rER)
Glycolysis
TCA cycle
Pgi
Pfk
Tpi
Gapdh
Pglym
Eno
Ldh
Cs
Idh
Scs
H
S. litura: hemolymph
ATP pmol/μl
Hours post-infection
Control
AcMNPV
BmNPV
Relative ADP/ATP ratio
B. mori: hemolymph
ATP pmol/μl
Hours post-infection
Control
AcMNPV
BmNPV
Relative ADP/ATP ratio
S. litura: fat body
ATP pmol/μl
Hours post-infection
Control
AcMNPV
BmNPV
Relative ADP/ATP ratio
B. mori: fat body
ATP pmol/μl
Hours post-infection
Control
AcMNPV
BmNPV
Relative ADP/ATP ratio

Figure 2. The effects of permissive and nonpermissive infection on glycolysis, TCA cycle pathways and energy production in *S. litura* and *B. mori* larvae

(A and B) *S. litura* (A) and *B. mori* (B) (n = 3) were infected with AcMNPV and BmNPV, and changes in glucose concentration in the hemolymph was determined at 0, 24, and 48 hpi.

(C and D) Changes in glucose concentration in the fat body of *S. litura* (C) and *B. mori* (D) were also determined. Data are represented as mean ± SD.

(E) Schematic of the glycolysis and TCA cycle pathways. Important metabolites and enzymes are labeled in black and red, respectively.

(F and G) Expression levels of metabolic genes involved in glycolysis and the TCA cycle were determined by RT-qPCR for *S. litura* and *B. mori* infected with AcMNPV and BmNPV for 24 h (F) and 48 h (G). Gene expression was specifically analyzed in the hemolymph and the fat body. Expression levels were normalized to that of the *18S* gene. Relative expression ratios (rER) to the uninfected control are presented as a color spectrum in a heat map in which red and green represent increased and decreased gene expression, respectively.

(H) ATP levels (at 0, 24, and 48 hpi) and relative ADP/ATP ratio (at 48 hpi) in larval tissues after AcMNPV or BmNPV infection. Results of ADP/ATP ratio were normalized to that of the uninfected control at 0 hpi. Data are represented as mean ± SD. The red line indicates the nonpermissive infection condition. Student's *t*-test was used to determine the statistical significance of any differences (*p <0.05; **p <0.01; ***p <0.005).

To verify the metabolic alteration in nonpermissively-infected larvae, we analyzed the expression of trehalases and glycogen phosphorylase, the principal enzymes that are involved in the conversion of trehalose and glycogen to glucose. Expression levels of soluble form trehalase, trehalase-1, were higher in the hemolymph of nonpermissive larvae [BmNPV-infected *S. litura* (Figure 1E) and AcMNPV-infected *B. mori* (Figure 1F)] compared to that of permissively-infected larvae. For the membrane-bound trehalase, trehalase-2, expression levels in the hemolymph showed no significant difference (Figure S2), correlating with previous findings that trehalase-1 is the major trehalase in the hemolymph (Gu et al., 2009; Shukla et al., 2014). As for glycogen phosphorylase, its expression in the fat body of nonpermissive larvae was also higher than in permissive larvae, especially at 48 hpi (Figures 1G and 1H), indicating that fat body glycogen was likely converted to trehalose or glucose after nonpermissive infection. The fact that no significant reduction was observed in fat body glycogen (Figures 1C and 1D) may be because of its high initial content. These results demonstrate that the host carbohydrate metabolism reacts differently to permissive and nonpermissive infections, and that the latter results in an increased consumption of stored sugars, specifically the early depletion of trehalose in the hemolymph followed by the conversion of glycogen in the fat body.

Nonpermissive infection upregulates glycolysis and ATP synthesis

Trehalase-1 and glycogen phosphorylase trigger the conversion of stored sugars into glucose. As such, we measured the glucose content in the hemolymph and fat body of larvae after viral infection. In the hemolymph of *S. litura* and *B. mori*, glucose content was significantly increased 24 h after non-permissive infection (Figures 2A and 2B). The same situation was found for fat body glucose in both species: at 24 hpi, the fat body glucose content was significantly higher in nonpermissively-infected larvae (Figures 2C and 2D). This increased glucose content subsequently decreased at 48 hpi (Figures 2A–2D), suggesting that the excess glucose may have undergone glycolysis or the TCA cycle to yield ATP for cellular functions. We analyzed the transcription level of seven enzymes in the glycolytic pathway and three enzymes in the TCA cycle (Figure 2E) in the hemolymph and fat body of the larvae. At 24 hpi, no significant changes were determined in the gene expression of most of the enzymes in both tissues under either permissive or nonpermissive infection regimens (Figure 2F and Tables S1 and S2), except for an increase of citrate synthase in the hemolymph of BmNPV-infected *S. litura* and a decrease of TCA cycle-related enzymes in the fat body of AcMNPV-infected *S. litura*. In contrast, at 48 hpi, expression levels of glycolysis and TCA cycle enzymes increased in the hemolymph of *B. mori*, especially in those with a nonpermissive infection (AcMNPV) (Figure 2G and Tables S3 and S4). The expression of these metabolic genes in the fat body of both larvae also increased more significantly under nonpermissive conditions (Figure 2G and Tables S3 and S4).

Next, we measured the concentration of ATP and the ratio of ADP/ATP in larval tissues. Because the sum of ATP + ADP is expected to remain constant, the decrease in ADP/ATP ratio reflected the conversion of ADP into ATP through glycolysis or the TCA cycle. Under all infection conditions, ATP increased with time in the hemolymph and the fat body; however, under nonpermissive conditions there was a more pronounced increment (Figure 2H). Consistently, the ADP/ATP ratio was found to markedly decrease at 48 hpi for all nonpermissive infections (Figure 2H). Taken together, these results indicate that the increased carbohydrate metabolism during nonpermissive infections produced more glucose in the tissues at around 24 hpi. The glucose content decreased at 48 hpi as glucose molecules entered the glycolytic pathway and TCA cycle to yield ATP.

Previous studies have indicated that glycolytic activity is regulated by adenosine signaling upon pathogen infection (Anderson et al., 1973; Bajgar and Dolezal, 2018; Lin et al., 2020). We examined the expression of adenosine receptor (AdoR) in the hemolymph and the fat body of both larvae after permissive and nonpermissive infections. The results showed that *AdoR* expression in the hemolymph of nonpermissively-infected larvae increased with time (Figures 3A and 3B), whereas no significant increase was determined in the fat body under either infection regimen (Figures 3C and 3D). To confirm the existence of increased adenosine signaling, we determined the level of extracellular adenosine in the hemolymph at 24 hpi. Adenosine content was found to be the highest for nonpermissive infections compared to permissive infections or uninfected controls (Figures 3E and 3F). Furthermore, the expression of *puckered* (*puc*) of the JNK pathway (Poernbacher and Vincent, 2018) and JAK/STAT ligands *unpaired 1* (*upd1*) and *upd2* (Xu et al., 2020) that are regulated downstream of the adenosine signaling were increased significantly following nonpermissive infection (Figure S3). These results demonstrate that adenosine signaling increased in the hemolymph of larvae after nonpermissive viral infection.

Nonpermissive infections induce stronger immune responses in the host than permissive infections

Typically, a permissive infection increases and utilizes the host energy to facilitate virus replication (Sanchez and Lagunoff, 2015). Considering that viruses cannot replicate in a nonpermissive host, as well as the occurrence of increased adenosine signaling (Figure 3), we speculated that the increased energy production in nonpermissive infections was triggered by the host for eliciting immune responses against the virus. To determine whether nonpermissive infections were consistent with an increased immune response, we examined both the cellular and humoral immunities of the infected larvae. Measurements for these immune responses were mostly conducted at 48 hpi because we assumed that virus-induced metabolic alterations exert more pronounced effects on the host's immunities at a later timing (relative to 24 hpi). For cellular immunity, we isolated hemocytes from larvae infected with the different viruses at 48 hpi and tested their capability to phagocytose *E. coli* bacteria. The results showed that hemocytes from the nonpermissive infection groups exhibited higher phagocytosis activity than those from the permissive infection groups, irrespective of the larval species [*S. litura* (Figures 4A and 4B), *B. mori* (Figures 4C and 4D)].

For humoral immunity, we determined the expression level of genes involved in humoral immunity pathways at 48 hpi, including four genes from the Toll pathway (*Toll*, *MyD88*, *Pelle*, and *Cactus*), three genes from the IMD pathway (*PGRP*, *FADD*, and *Relish*), and three genes from the JAK/STAT pathway (*HOP*, *STAT*, and *Pi3k60*). In *S. litura*, the expression levels of these ten genes reduced or remained unchanged after permissive infection (AcMNPV) but increased after nonpermissive infection (BmNPV) (Figure 4E). In *B. mori*, the expression levels of most genes increased after permissive infection (BmNPV) (Figure 4E). This increase in expression became significant after nonpermissive infection (AcMNPV) (Figure 4E). These results indicate that non-permissive infection stimulates or boosts the expression of most genes involved in the immune pathways for both *S. litura* and *B. mori*.

The activation of Toll, IMD, and JAK/STAT pathways triggers the production of AMPs such as gloverin (Figure 4F). So far, one and four types of gloverin have been identified in *S. litura* and *B. mori* (i.e., Gloverins 1–4), respectively. We measured the expression levels of these gloverin genes in the respective larvae. In *S. litura*, no significant difference was found in gloverin expression at 24 hpi for either AcMNPV or BmNPV infection ($p = 0.28$); however, at 48 hpi, expression in BmNPV-infected *S. litura* (nonpermissive infection) was significantly higher than that of AcMNPV-infected larvae (permissive infection) ($p = 0.0005$) (Figure 4G). This trend of gloverin expression was similar in *B. mori*: *gloverin-1* and *gloverin-4* showed significantly higher expression in the nonpermissive infection groups (AcMNPV) compared to permissive infection groups (BmNPV) at 48 hpi (Figure 4H), with the difference in *gloverin-4* expression being the most statistically significant ($p = 0.01$) (Figure 4H). Altogether, these results suggest that nonpermissive infection induces a stronger immune response in the host, including increased phagocytosis, immune gene expression, and AMP production at the late stage of infection.

Inhibition in glycolysis or immune response enhances baculovirus replication in nonpermissive hosts

The above results demonstrate that nonpermissive infection by baculoviruses increases the host's carbohydrate metabolism and yields more ATP, in parallel with an increased immune response. To confirm that this increased metabolism is induced by the host to enhance its response against virus replication

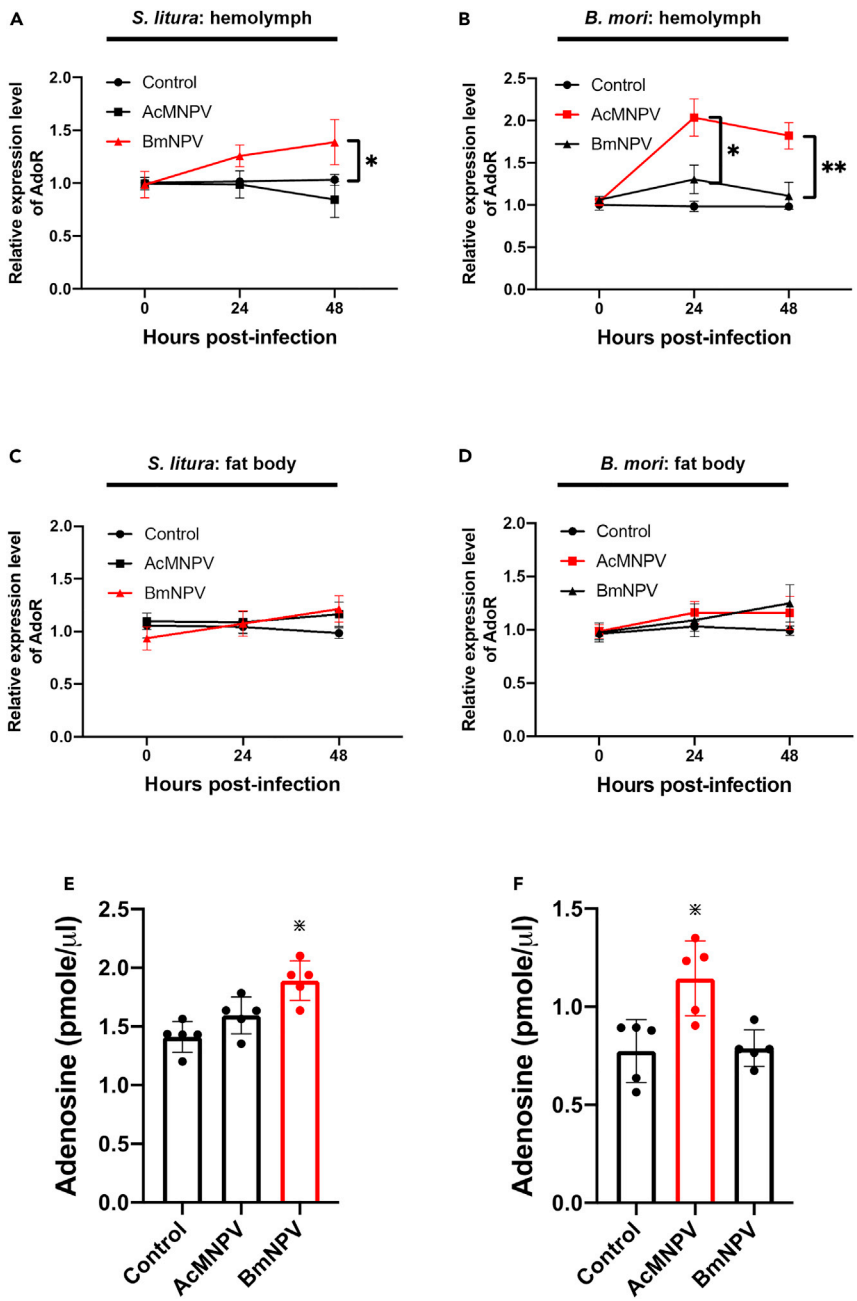

Figure 3. Regulation of adenosine signaling upon permissive and nonpermissive infections

(A–D) RT-qPCR analyses of *AdoR* expression in the hemolymph of *S. litura* (A) and *B. mori* (B), and in the fat body of *S. litura* (C) and *B. mori* (D) were determined at 0, 24, and 48 hpi for both AcMNPV and BmNPV infection. Data for each condition are normalized to the expression of the *18S* gene and expressed as a relative ratio to the uninfected control.

(E and F) The changes in adenosine concentration in the hemolymph of *S. litura* (E) and *B. mori* (F) were determined at 24 hpi for both AcMNPV and BmNPV infection. All values are shown as the mean ± SD of three replicates for qPCR and four replicates for adenosine measurement. Student's *t* test was used to determine statistically significant differences (*p <0.05; **p <0.01) between permissive and nonpermissive infections for *AdoR* expression (A–D) or between the nonpermissive infection and the uninfected control for adenosine content (E and F). Red lines indicate the nonpermissive infection condition.

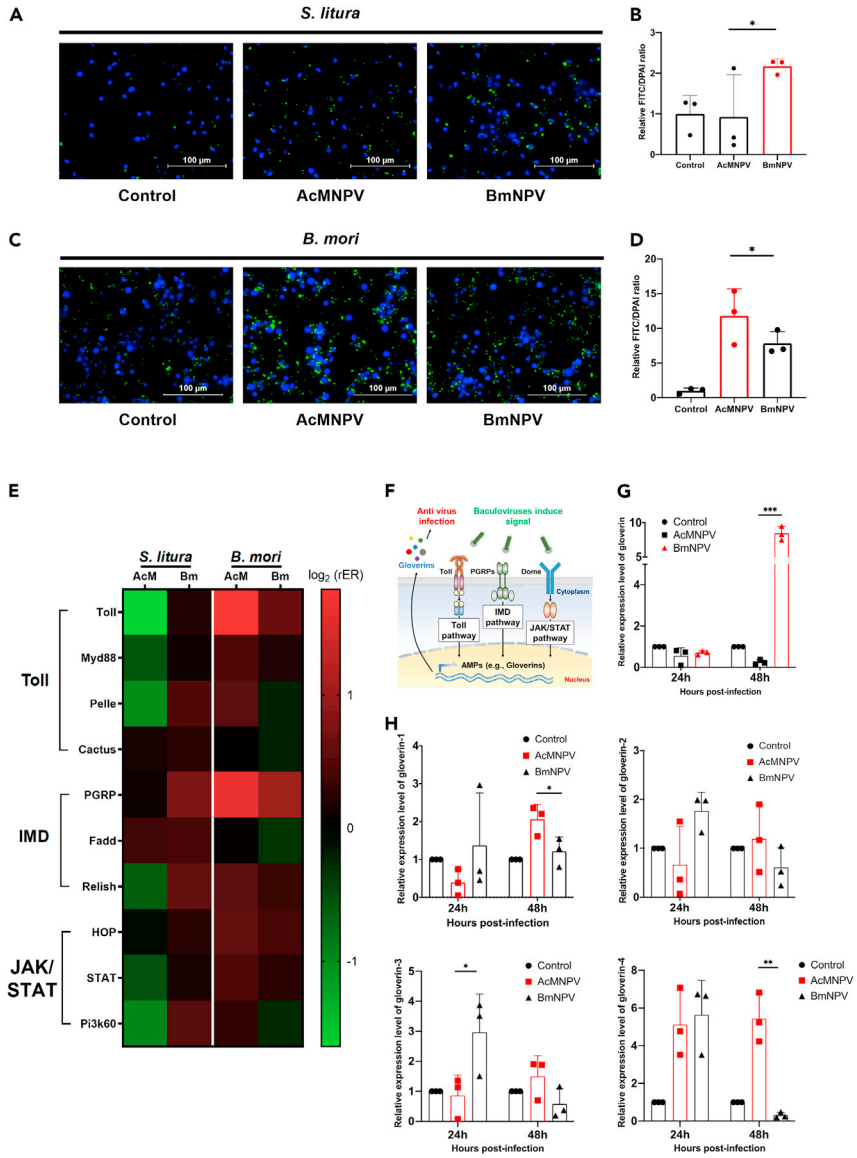

Figure 4. Determination of cellular and humoral immune responses in *S. litura* and *B. mori* larvae after permissive and nonpermissive infections

Larvae (n = 3) of *S. litura* and *B. mori* were infected with AcMNPV and BmNPV. Larval lymphocytes were isolated at 48 hpi and their phagocytosis activity was determined by the engulfment of FITC-labeled *E. coli*. Green fluorescence (FITC): FITC-labeled *E. coli*. Blue fluorescence (DAPI): hemocyte nuclei. (A) Representative images of *S. litura* lymphocytes without virus infection or with different virus infections. Bars: 100 μm.

(B) Quantification of phagocytosis activity of *S. litura* lymphocytes by the relative fold change in the FITC/DAPI fluorescence intensity ratio compared to the uninfected control.

(C) Representative images of *B. mori* lymphocytes. Bars: 100 μm.

(D) Quantification of the phagocytosis activity of *B. mori* lymphocytes.

(E) Changes in the expression level of humoral immunity pathway genes were determined at 48 hpi by RT-qPCR. Expression levels were normalized to that of the *18S* gene. rER to the uninfected control are presented as a heat map in which red and green represent increased and decreased gene expression, respectively.

(F) Schematic showing that baculoviruses activate signal transduction in the host's humoral immune pathways (i.e., Toll, IMD, and JAK/STAT), leading to the expression of AMPs (e.g., gloverins) that facilitate antiviral responses.

(G and H) The expression level of *gloverin* (G) in *S. litura* (n = 3) and *gloverin-1*, *gloverin-2*, *gloverin-3*, and *gloverin-4* in *B. mori* (H), was determined by RT-qPCR at 24 and 48 h after AcMNPV and BmNPV infections. Levels were normalized to that of the *18S* gene and the data expressed relative to the uninfected control. All data are represented as mean ± SD. Student's *t*-test was used to determine the statistical significance of any differences (*p <0.05; **p <0.01; ***p <0.005).

during a nonpermissive infection, we inhibited glycolysis or the immune response in the host and determined the effects on virus replication. Glycolysis inhibition was achieved by treating the *S. litura* cell line, SL1A, and the *B. mori* cell line, BmN, or either larvae, with glycolytic inhibitor 2-deoxy-D-glucose (2DG). The results of the cytotoxicity assay showed that 2DG at a concentration of up to 50 mM did not cause significant cell death within 72 h (Figure S4). For larvae, 2DG treatment (10 mM) did not lead to higher mortality than with untreated larvae after 5 days (Figure S5). The treatment of 10 mM of 2DG in cells and larvae significantly reduced the expression of glycolytic genes (Figure S6) and subsequent ATP production (Figures 5A–5D). After infecting cells and larvae with the viruses for 48 h, we analyzed the production of virus progeny in the cell supernatant and larval body fluid. For the permissive infection of AcMNPV, the addition of 2DG did not cause a significant difference in the viral titer in SL1A cells; however, it was significantly increased during the nonpermissive infection of BmNPV (Figure 5E). Similar results were observed in the BmN cells, namely that 2DG treatment increased the viral titer after nonpermissive infection (AcMNPV) (Figure 5F). Furthermore, in larvae injected with 2DG-mixing viruses, the viral titer in nonpermissive infections (*S. litura*: BmNPV; *B. mori*: AcMNPV) increased in the body fluid, whereas the viral titer in permissive infections (*S. litura*: AcMNPV; *B. mori*: BmNPV) barely changed (Figures 5G and 5H). These results indicate that the increased level of host energy during nonpermissive infection is not used to support virus replication but instead has an inhibitory effect.

To elucidate the effect of host immunity on determining whether an infection is permissive or nonpermissive, we inhibited the transcription of gloverin in SL1A and BmN cells. The transfection of respective gloverin siRNA (Figure S7A) successfully induced RNAi that decreased transcription of the gloverin gene in SL1A and BmN cells (Figures S7B and S7C). We infected the cells with recombinant viruses expressing an enhanced green fluorescent protein (EGFP). At 48 hpi, the expression of EGFP remained approximately the same in control cells or those treated with gloverin siRNA under a permissive infection regimen; however, under a nonpermissive infection regimen, cells treated with gloverin siRNA exhibited increased EGFP expression (Figures 6A and 6B). When measuring the viral titer in the culture supernatant, no significant change was found in the control or siRNA treatment groups with permissive infections, whereas the viral titer increased significantly under the gloverin RNAi condition in the nonpermissive infection groups (Figures 6C and 6D). These results indicate that gloverin production is a means by which the host inhibits nonpermissive infection. Taken together, our data show that viruses are able to infect a nonpermissive host when the host has inadequate energy to trigger an immune response. Conversely, switching energy to mount immune responses in a nonpermissive host blocks infection by these viruses. In other words, the metabolic switch of the host is a determinant for virus infectivity.

DISCUSSION

In previous studies, the regulation of AcMNPV and BmNPV host tropism has largely focused on viral factors, rather than the host's responses after infection. Therefore, in the present study, we investigated changes to the carbohydrate metabolism of *S. litura* and *B. mori* larvae after both permissive and nonpermissive infections. We found a greater depletion of stored carbohydrates followed by increased energy production in larvae subjected to nonpermissive infections. Although viruses in permissive infections were also found to alter the host's metabolic pathways to produce energy for replication, our results showed that the excess energy generated during nonpermissive infections was redirected to the immune system to inhibit virus replication and propagation. The host specificity of a virus may not be attributed to a single factor and our study provides evidence that the switch in carbohydrate metabolism is one of such decisive factors that shape the host tropism of a virus.

Several viral factors have previously been identified as influencing baculovirus host specificity. Glycoprotein GP64 of BmNPV was found to prevent the virion from transporting into the nucleus of nonpermissive *S. litura* and *T. ni* cell lines (Katou et al., 2006). BmNPV P143 is vital for the assembly or release of virus particles in *B. mori* and thus replacing AcMNPV P143 with BmNPV P143 (Croizier et al., 1994) or substituting specific amino acids on AcMNPV P143 (Argaud et al., 1998; Croizier et al., 1994; Nagamine and Sako, 2016) enables AcMNPV to replicate in *B. mori* larvae or cell lines. Such factors also include HRF-1 (Thiem et al., 1996) and HCF-1 (Tachibana et al., 2017), which enhance viral DNA replication and viral protein synthesis in certain cell lines. These studies focused on how viral factors influence the viral multiplication process in a host and revealed that the functionality of a single viral factor may not be able to ease the constraints for all nucleopolyhedroviruses (NPVs) in a nonpermissive host (Tachibana et al., 2017). A permissive and nonpermissive host may exert different effects on a virus. In the present study, we found

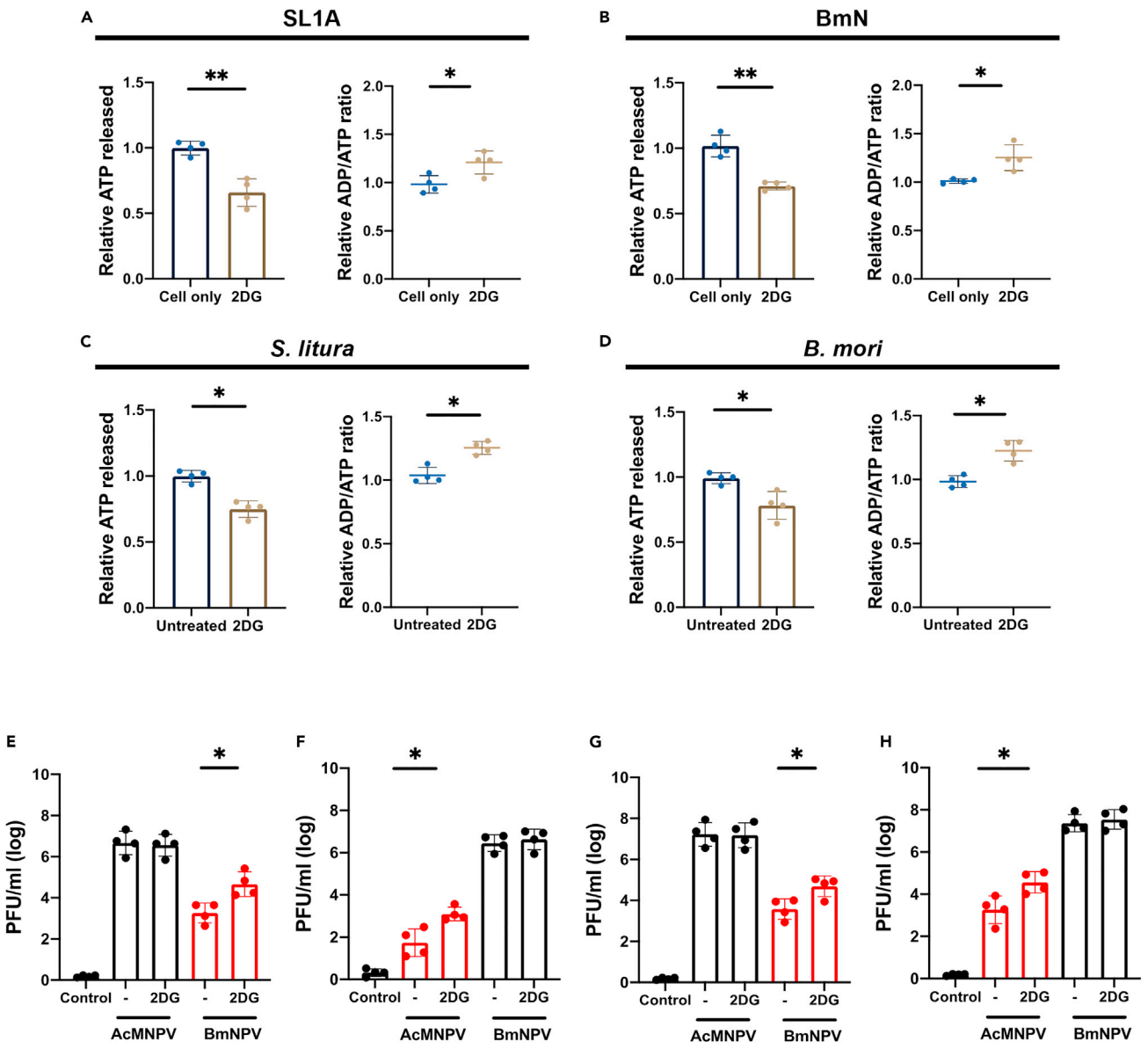

Figure 5. Inhibition of glycolysis by 2DG treatment and its effects on energy production and the infectivity of AcMNPV and BmNPV in permissive and nonpermissive cell lines and larvae

(A and B) Cell lines SL1A (A) and BmN (B) were treated with 10 mM 2DG for 48 h. The amount of released ATP and the ADP/ATP ratio were measured in the cell supernatant and compared to those of the untreated control.

(C and D) Larvae of S. litura (C) and *B. mori* (D) were injected with 10 mM 2DG and examined after 48 h. The amount of released ATP and the ADP/ATP ratio were measured in the body fluid and compared to the untreated control.

(E and F) The infectivity of AcMNPV and BmNPV in cell lines SL1A (E) and BmN (F) with or without 2DG treatment were determined by measuring the viral titer in culture supernatants at 48 hpi.

(G and H) The infectivities of AcMNPV and BmNPV in *S. litura* (G) and *B. mori* (H) larvae with or without 2DG injection were also determined by measuring the viral titer in body fluids at 48 hpi. Red bars indicate nonpermissive infection conditions. All data are represented as mean ± SD. Student's *t*-test was used to determine the statistical significance of any differences (*p <0.05, **p <0.01).

that the carbohydrate metabolism significantly differed between permissively-infected and nonpermissively-infected *S. litura* and *B. mori*. The concentration of trehalose decreased in the host's hemolymph after nonpermissive infection, alongside an increased expression of trehalase-1 and glycogen phosphorylase (Figure 1). These results indicate a highly active conversion of stored sugars into monosaccharides following a nonpermissive infection; our analyses of the glucose content indeed displayed an increase in

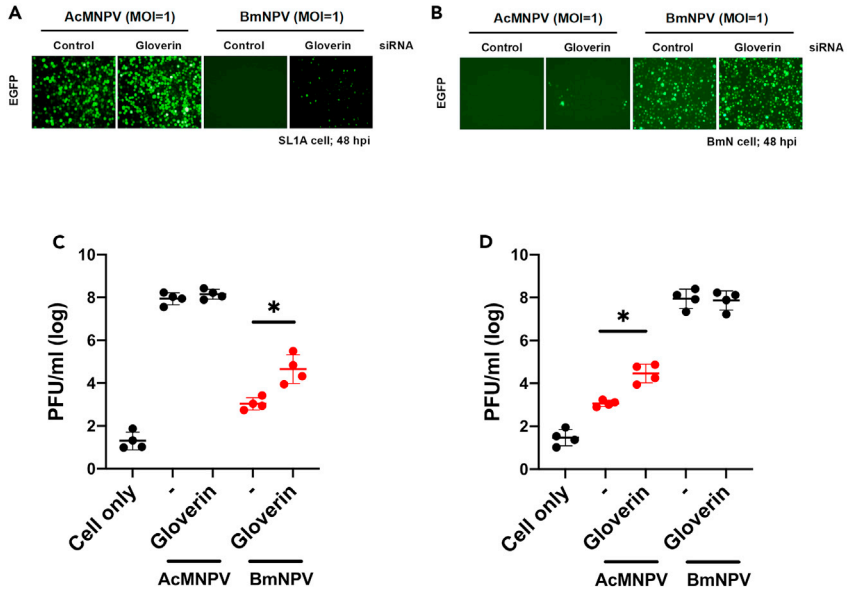

Figure 6. Inhibition of gloverin expression by siRNA treatment and its effects on the infectivity of AcMNPV and BmNPV in permissive and nonpermissive cell lines

(A and B) Cell lines SL1A (A) and BmN (B) were treated with siRNA of the respective gloverin (*gloverin-4* for BmN cells) or siRNA-control and infected with recombinant AcMNPV and BmNPV carrying an EGFP reporter at 24 h post-transfection (hpt) of siRNA. Infectivity of the viruses was determined by EGFP expression in cells at 48 hpi. Representative images of fluorescent microscopy are presented.

(C and D) Viral titer in culture supernatants of SL1A (C) and BmN (D) treated with siRNA-gloverin or siRNA-control were also determined. Red indicates nonpermissive infections. Data are represented as mean ± SD. Student's *t*-test was used to determine the statistical significance of any differences (*p <0.05)

both the hemolymph and fat body, 24 h after nonpermissive infection (Figures 2A–2D). The excessive glucose became the carbon source for cellular respiration as the decrease in glucose content at 48 hpi coincided with an increased expression of enzymes involved in glycolysis or the TCA cycle (Figure 2G). Finally, the significantly elevated ATP level and lowered ADP/ATP ratio found in nonpermissively-infected compared to permissively-infected larvae (Figure 2H) support the former observed metabolic changes. These phenomena were present in both *S. litura* and *B. mori* larvae, indicating that increased energy demand may be common when lepidopteran insects encounter a nonpermissive baculovirus infection.

Viruses are obligate parasites that rely on the energy provided by the host for replication and propagation. Metabolic alterations in the host during infection are thus a strategy for viruses to sustain their replication. Many viruses induce glycolysis in host cells to produce glucose as a carbon source, such as with human cytomegalovirus (HCMV), herpes simplex virus type-1 (HSV-1), and poliovirus (Sanchez and Lagunoff, 2015). Other metabolic alterations include increased lipid synthesis (Dias et al., 2020; Vastag et al., 2011), pyrimidine synthesis (Vastag et al., 2011), and glutaminolysis (Fontaine et al., 2014). Similar metabolic alterations have also been observed in insects. For example, when a persistent infection of Cricket paralysis virus (CrPV) in silkworm Bm5 cells progresses into its pathogenic stages, glucose and glutamine levels significantly decrease to fuel virus replication and virion production (Wang et al., 2019). In contrast, when CrPV causes acute infection in *Drosophila* S2 cells, the overall alteration to amino acid and carbohydrate levels was observed to be smaller than that in Bm5 cells, suggesting that these resources were more sufficient in S2 cells to trigger an acute infection (Wang et al., 2020). In our results, permissive infections exhibited relatively few alterations in the host carbohydrate metabolism compared to that during nonpermissive infections (Figures 1 and 2). However, in the case of nonpermissive infection, the increased carbohydrate metabolism did not provide energy for virus infection, as reflected by the low virus yields. Moreover, when glycolysis was blocked by 2DG in nonpermissive cells or larvae, the viral titer increased in the supernatant or body fluid (Figure 5). This result is exactly opposite to that previously observed in glycolysis-inducing viruses that alter host glycolysis for virus propagations; in these cases 2DG inhibited the propagation of glycolysis-inducing viruses instead (Sanchez and Lagunoff, 2015). Hence, our results

show that the induced carbohydrate metabolism in nonpermissive infections may not be an alteration implemented by the viruses to obtain resources from the host, but are more likely an antiviral response of the host to resist infection.

In mammals, the activation of immune cells (e.g., macrophages) requires massive amounts of energy, and thus metabolic changes such as increasing glycolysis and lipid synthesis and modulating of the TCA cycle may take place (Palsson-McDermott and O'neill, 2013; Van den Bossche et al., 2017). In insects, the stimulation of immune cell activity also increases energy demand. For instance, glucose consumption in *Drosophila* immune cells increased from 11% to 27% (of total glucose) during infection by a parasitoid (Bajgar et al., 2015). We speculated that the energy generated in nonpermissive larvae was redirected to activate immune responses. In insects, adenosine signaling is known to regulate glycolytic activity after pathogenic infection. Overexpression of AdoR or adding adenosine activates the immune responses mediated by the JNK and JAK/STAT pathways (Poernbacher and Vincent, 2018; Xu et al., 2020). In our previous study, we found that inhibiting adenosine signaling not only decreased ATP synthesis but also decreased AMP expression, eventually contributing to increased virus progeny (Lin et al., 2020). Accordingly, adenosine and its signaling pathway might mediate the increased energy production and antiviral responses in nonpermissive infections. We determined an increase in *AdoR* expression in the hemolymph but not the fat body of larvae under nonpermissive infections (Figures 3A–3D). These results correlate with a previous transcriptome analysis which indicated that *AdoR* expression is tissue-specific (Jiang et al., 2016). Increased adenosine content (Figures 3E and 3F) and the upregulated expression of genes downstream of the signaling (Figure S3) demonstrated that adenosine signaling occurred in the hemolymph of nonpermissively-infected larvae. Subsequently, larvae also exhibited increased cellular immunity after nonpermissive infection, as reflected by phagocytosis activity (Figures 4A–4D). Humoral immunity was also stimulated in the host after nonpermissive infection, reflected in an increase in the expression of humoral immunity genes in the Toll, IMD, and JAK/STAT pathways (Figure 4E). Moreover, expression of the *S. litura* gloverin gene and two *B. mori* gloverin genes increased significantly in nonpermissive infections (Figures 4G and 4H). To prove that gloverin expression indeed inhibited virus replication in nonpermissive hosts, we used siRNA to inhibit gloverin expression in cells (as the efficiency of RNAi in larvae is still poor). Viral replication was significantly increased in nonpermissive cells with gloverin gene knockdown (Figure 6), supporting the involvement of gloverin in nonpermissive infections.

Host specificity is likely regulated by more factors than explored herein, because the inhibition of glycolysis or the immune response did not fully elevate the virus titer in nonpermissive infections to that exhibited in permissive infections (Figures 5 and 6). It will be interesting to examine whether recombinant baculoviruses carrying previously characterized mutations (Croizier et al., 1994; Katou et al., 2006) can infect their nonpermissive hosts but elicit lower metabolic alterations compared to wild-type viruses. Our present study provides a new insight, namely that the host's physiological responses can affect virus infectivity. In summary, when baculoviruses infect a permissive host, viruses partially divert energy from the host without inducing significant changes in the carbohydrate metabolism or activating its immune systems (Figure 7, top). In contrast, when baculoviruses invade a nonpermissive host, the host's carbohydrate metabolism undergoes significant alteration: more energy is produced to mount an immune response, thereby inhibiting virus replication and propagation (Figure 7, bottom). Because we used AcMNPV and BmNPV that cause a nonpermissive infection in one another's permissive host(s), our study suggests that alteration of carbohydrate metabolism may be a ubiquitous mechanism mediated by lepidopteran insects against nonpermissive infection. This finding may thus assist future investigations of baculovirus infections and contribute to the effective management of lepidopteran pests.

Limitations of the study

In this study, we revealed the role of host metabolism in determining permissive and nonpermissive infections of baculoviruses. Nevertheless, there are still some unresolved issues. First, we did not precisely trace the mobilization of carbohydrates in tissues through methods such as isotope labeling, which can provide direct evidence for metabolic switches during virus infections. Second, alterations in other metabolic pathways (e.g., lipid metabolic pathway) were not discussed in the study. Exploring the associated changes in carbohydrate metabolism and other metabolisms can elucidate more thorough alterations in host metabolisms. Finally, previously identified virus factors that expand the host range have not yet been integrated with the effects of metabolic alterations. Future studies using recombinant viruses bearing related mutations may help to link viral genetics to these host physiologic regulations.

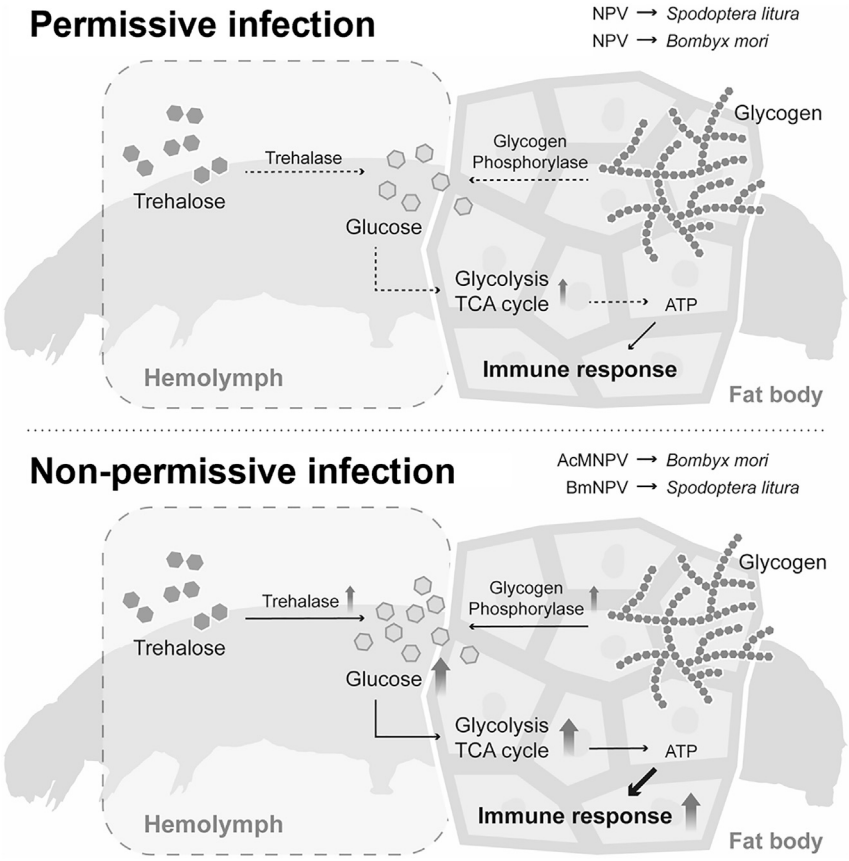

Figure 7. Illustration of how alteration in carbohydrate metabolism leads to permissive and nonpermissive infections in *S. litura* and *B. mori* larvae

In permissive infections (top), carbohydrate metabolisms are barely affected and relatively weak immune responses are elicited. In nonpermissive infections (bottom), trehalose in the hemolymph and glycogen in the fat body are converted by trehalase-1 and glycogen phosphorylase, respectively, into significant amounts of glucose. Metabolism pathways, including glycolysis and the TCA cycle, are fueled by the excessive glucose and produce more ATP for the subsequent immune responses. The enhanced immune responses inhibit the replication and propagation of the virus and therefore lead to nonpermissive infections.

STAR★METHODS

Detailed methods are provided in the online version of this paper and include the following:

- KEY RESOURCES TABLE
- RESOURCE AVAILABILITY
  - Lead contact
  - Materials availability
  - Data and code availability
- EXPERIMENTAL MODEL AND SUBJECT DETAILS
  - Insects
  - Cells and viruses
- METHOD DETAILS
  - Measurement of trehalose, glycogen, glucose, and adenosine in tissues
  - Analysis of gene expression by RT-qPCR
  - ATP and ADP/ATP ratio analyses
  - Phagocytosis assay
  - Treatment of 2DG in cells and larvae
  - siRNA transfection
- QUANTIFICATION AND STATISTIC ANALYSIS

SUPPLEMENTAL INFORMATION

Supplemental information can be found online at https://doi.org/10.1016/j.isci.2021.103648.

ACKNOWLEDGMENTS

We thank Mr. Alexander Barton for kindly revising the English language of the manuscript. This research was funded by the grant MOST 107-2311-B-002-024-MY3 to Y.L.W. from the Ministry of Science and Technology, Taiwan.

AUTHOR CONTRIBUTIONS

C.H.T., Y.C.C., Y.H.L., and Y.L.W. designed research; Y.C.C., C.Y.L., C.K.T., and Y.L.W. performed research; C.H.T., Y.C.C., S.C.W., and Y.L.W. analyzed data; and C.H.T. and Y.L.W. wrote the paper.

DECLARATION OF INTERESTS

The authors declare no competing interests.

Received: June 1, 2021
Revised: October 14, 2021
Accepted: December 15, 2021
Published: January 21, 2022

REFERENCES

Anderson, R.S., Holmes, B., and Good, R.A. (1973). Comparative biochemistry of phagocytizing insect hemocytes. Comp. Biochem. Physiol. B. *46*, 595–602.

Argaud, O., Croizier, L., López-Ferber, M., and Croizier, G. (1998). Two key mutations in the host-range specificity domain of the p143 gene of Autographa californica nucleopolyhedrovirus are required to kill *Bombyx mori* larvae. J. Gen. Virol. *79*, 931–935. https://doi.org/10.1099/0022-1317-79-4-931.

Bajgar, A., and Dolezal, T. (2018). Extracellular adenosine modulates host-pathogen interactions through regulation of systemic metabolism during immune response in *Drosophila*. PLoS Pathog. *14*, e1007022. https://doi.org/10.1371/journal.ppat.1007022.

Bajgar, A., Kucerova, K., Jonatova, L., Tomcala, A., Schneedorferova, I., Okrouhlik, J., and Dolezal, T. (2015). Extracellular adenosine mediates a systemic metabolic switch during immune response. PLoS Biol. *13*, e1002135.

Bao, Y.-Y., Tang, X.-D., Lv, Z.-Y., Wang, X.-Y., Tian, C.-H., Xu, Y.P., and Zhang, C.-X. (2009). Gene expression profiling of resistant and susceptible *Bombyx mori* strains reveals nucleopolyhedrovirus-associated variations in host gene transcript levels. Genomics *94*, 138–145. https://doi.org/10.1016/j.ygeno.2009.04.003.

Bartholomay, L.C., Cho, W.-L., Rocheleau, T.A., Boyle, J.P., Beck, E.T., Fuchs, J.F., Liss, P., Rusch, M., Butler, K.M., and Wu, R.C.-C. (2004). Description of the transcriptomes of immune response-activated hemocytes from the mosquito vectors *Aedes aegypti* and *Armigeres subalbatus*. Infect. Immun. *72*, 4114–4126.

Becker, A., Schlöder, P., Steele, J., and Wegener, G. (1996). The regulation of trehalose metabolism in insects. Experientia *52*, 433–439.

Blandin, S., and Levashina, E.A. (2004). Thioester-containing proteins and insect immunity. Mol. Immunol. *40*, 903–908.

Van den Bossche, J., O'Neill, L.A., and Menon, D. (2017). Macrophage immunometabolism: where are we (going)? Trends Immunol. *38*, 395–406.

Bretscher, A.J., Honti, V., Binggeli, O., Burri, O., Poidevin, M., Kurucz, E., Zsamboki, J., Ando, I., and Lemaitre, B. (2015). The Nimrod transmembrane receptor eater is required for hemocyte attachment to the sessile compartment in *Drosophila melanogaster*. Biol. Open *4*, 355–363. https://doi.org/10.1242/bio.201410595.

Chang, Y., Tang, C.-K., Lin, Y.-H., Tsai, C.-H., Lu, Y.-H., and Wu, Y.-L. (2020). Snellenius manilae bracovirus suppresses the host immune system by regulating extracellular adenosine levels in *Spodoptera litura*. Sci. Rep. *10*, 1–11.

Chen, Y.W., Wu, C.P., Wu, T.C., and Wu, Y.L. (2018). Analyses of the transcriptome of *Bombyx mori* cells infected with either BmNPV or AcMNPV. J. Asia Pac. Entomol. *21*, 37–45. https://doi.org/10.1016/j.aspen.2017.10.009.

Croizier, G., Croizier, L., Argaud, O., and Poudevigne, D. (1994). Extension of Autographa californica nuclear polyhedrosis virus host range by interspecific replacement of a short DNA sequence in the p143 helicase gene. Proc. Natl. Acad. Sci. U S A *91*, 48–52.

Crozatier, M., Ubeda, J.-M., Vincent, A., and Meister, M. (2004). Cellular immune response to parasitization in *Drosophila* requires the EBF orthologue collier. PLoS Biol. *2*, e196.

DiAngelo, J.R., Bland, M.L., Bambina, S., Cherry, S., and Birnbaum, M.J. (2009). The immune response attenuates growth and nutrient storage in *Drosophila* by reducing insulin signaling. Proc. Natl. Acad. Sci. U S A *106*, 20853–20858.

Dias, S.S.G., Soares, V.C., Ferreira, A.C., Sacramento, C.Q., Fintelman-Rodrigues, N., Temerozo, J.R., Teixeira, L., Nunes da Silva, M.A., Barreto, E., Mattos, M., et al. (2020). Lipid droplets fuel SARS-CoV-2 replication and production of inflammatory mediators. PLoS Pathog. *16*, e1009127. https://doi.org/10.1371/journal.ppat.1009127.

Dolezal, T., Krejcova, G., Bajgar, A., Nedbalova, P., and Strasser, P. (2019). Molecular regulations of metabolism during immune response in insects. Insect Biochem. Mol. Biol. *109*, 31–42.

Ferrandon, D., Jung, A., Criqui, M.C., Lemaitre, B., Uttenweiler-Joseph, S., Michaut, L., Reichhart, J.M., and Hoffmann, J. (1998). A drosomycin–GFP reporter transgene reveals a local immune response in *Drosophila* that is not dependent on the Toll pathway. EMBO J. *17*, 1217–1227.

Fontaine, K.A., Camarda, R., and Lagunoff, M. (2014). Vaccinia virus requires glutamine but not glucose for efficient replication. J. Virol. *88*, 4366–4374. https://doi.org/10.1128/jvi.03134-13.

Gillespie, J.P., Kanost, M.R., and Trenczek, T. (1997). Biological mediators of insect immunity. Annu. Rev. Entomol. *42*, 611–643.

Gomi, S., Majima, K., and Maeda, S. (1999). Sequence analysis of the genome of Bombyx mori nucleopolyhedrovirus. J. Gen. Virol. *80*, 1323–1337.

Groner, A. (1986). Specificity and safety of baculoviruses. In The biology of Baculoviruses: Biological properties and molecular Biology, R.R. Granados and B.A. Federici, eds. (CRC Press), pp. 177–202.

Gu, J., Shao, Y., Zhang, C., Liu, Z., and Zhang, Y. (2009). Characterization of putative soluble and membrane-bound trehalases in a hemipteran insect, Nilaparvata lugens. J. Insect Physiol. *55*,

997–1002. https://doi.org/10.1016/j.jinsphys.2009.07.003.

Hu, Y.T., Tang, C.K., Wu, C.P., Wu, P.C., Yang, E.C., Tai, C.C., and Wu, Y.L. (2018). Histone deacetylase inhibitor treatment restores memory-related gene expression and learning ability in neonicotinoid-treated *Apis mellifera*. Insect Mol. Biol. *27*, 512–521. https://doi.org/10.1111/imb.12390.

Jiang, L., Peng, Z., Guo, Y., Cheng, T., Guo, H., Sun, Q., Huang, C., Zhao, P., and Xia, Q. (2016). Transcriptome analysis of interactions between silkworm and cytoplasmic polyhedrosis virus. Sci. Rep. *6*, 24894. https://doi.org/10.1038/srep24894.

Katou, Y., Ikeda, M., and Kobayashi, M. (2006). Abortive replication of Bombyx mori nucleopolyhedrovirus in Sf9 and high five cells: defective nuclear transport of the virions. Virology *347*, 455–465.

Kondo, A., and Maeda, S. (1991). Host range expansion by recombination of the baculoviruses Bombyx mori nuclear polyhedrosis virus and autographa californica nuclear polyhedrosis virus. J. Virol. *65*, 3625–3632.

Koul, O., Shankar, J.S., Mehta, N., Taneja, S.C., Tripathi, A.K., and Dhar, K.L. (1997). Bioefficacy of crude extracts of *Aglaia* species (Meliaceae) and some active fractions against lepidopteran larvae. J. Appl. Entomol. *121*, 245–248. https://doi.org/10.1111/j.1439-0418.1997.tb01400.x.

Lin, Y.-H., Tai, C.-C., Brož, V., Tang, C.-K., Chen, P., Wu, C.P., Li, C.-H., and Wu, Y.-L. (2020). Adenosine receptor modulates permissiveness of baculovirus (budded virus) infection via regulation of energy metabolism in *Bombyx mori*. Front. Immunol. *11*, 763.

Lo, H.-R., and Chao, Y.-C. (2004). Rapid titer determination of baculovirus by quantitative real-time polymerase chain reaction. Biotechnol. Prog. *20*, 354–360.

Moreno-Habel, D.A., Biglang-awa, I.M., Dulce, A., Luu, D.D., Garcia, P., Weers, P.M., and Haas-Stapleton, E.J. (2012). Inactivation of the budded virus of Autographa californica M nucleopolyhedrovirus by gloverin. J. Invertebr. Pathol. *110*, 92–101.

Morishima, I., Horiba, T., Iketani, M., Nishioka, E., and Yamano, Y. (1995). Parallel induction of cecropin and lysozyme in larvae of the silkworm, *Bombyx mori*. Dev. Comp. Immunol. *19*, 357–363.

Nagamine, T., and Sako, Y. (2016). A role for the anti-viral host defense mechanism in the phylogenetic divergence in baculovirus evolution. PLoS One *11*, e0156394. https://doi.org/10.1371/journal.pone.0156394.

Palsson-McDermott, E.M., and O'neill, L.A. (2013). The Warburg effect then and now: from cancer to inflammatory diseases. Bioessays *35*, 965–973.

Poernbacher, I., and Vincent, J.-P. (2018). Epithelial cells release adenosine to promote local TNF production in response to polarity disruption. Nat. Commun. *9*, 4675. https://doi.org/10.1038/s41467-018-07114-z.

Sakurai, M., Shikata, M., Sano, Y., Hashimoto, Y., and Matsumoto, T. (1998). Virulence of autographs californica nucleopolyhedrovirus infection of non-permissive cultured cells of the silkworm, *Bombyx mori*. J. Seric. Sci. Jpn. *67*, 211–216.

Sanchez, E.L., and Lagunoff, M. (2015). Viral activation of cellular metabolism. Virology *479-480*, 609–618. https://doi.org/10.1016/j.virol.2015.02.038.

Schmittgen, T.D., and Livak, K.J. (2008). Analyzing real-time PCR data by the comparative C-T method. Nat. Protoc. *3*, 1101–1108. https://doi.org/10.1038/nprot.2008.73.

Shukla, E., Thorat, L.J., Nath, B.B., and Gaikwad, S.M. (2014). Insect trehalase: physiological significance and potential applications. Glycobiology *25*, 357–367. https://doi.org/10.1093/glycob/cwu125.

Singh, T., Singh, P.K., and Sahaf, K.A. (2013). Egg diapause and metabolic modulations during embryonic development in the silkworm, *Bombyx mori* L. (Lepidoptera: Bombycidae). Ann. Biol. Res. *4*, 12–21.

Song, C., Zhu, C., Wu, Q., Qi, J., Gao, Y., Zhang, Z., Gaur, U., Yang, D., Fan, X., and Yang, M. (2017). Metabolome analysis of effect of aspirin on *Drosophila* lifespan extension. Exp. Gerontol. *95*, 54–62. https://doi.org/10.1016/j.exger.2017.04.010.

Steele, J. (1982). Glycogen phosphorylase in insects. Insect Biochem. *12*, 131–147.

Strand, M.R., and Pech, L.L. (1995). Immunological basis for compatibility in parasitoid-host relationships. Annu. Rev. Entomol. *40*, 31–56.

Tachibana, A., Hamajima, R., Tomizaki, M., Kondo, T., Nanba, Y., Kobayashi, M., Yamada, H., and Ikeda, M. (2017). HCF-1 encoded by baculovirus AcMNPV is required for productive nucleopolyhedrovirus infection of non-permissive Tn368 cells. Sci. Rep. *7*, 3807. https://doi.org/10.1038/s41598-017-03710-z.

Thiem, S.M., Du, X., Quentin, M.E., and Berner, M.M. (1996). Identification of baculovirus gene that promotes autographa californica nuclear polyhedrosis virus replication in a nonpermissive insect cell line. J. Virol. *70*, 2221–2229.

Tzou, P., Ohresser, S., Ferrandon, D., Capovilla, M., Reichhart, J.-M., Lemaitre, B., Hoffmann, J.A., and Imler, J.-L. (2000). Tissue-specific inducible expression of antimicrobial peptide genes in *Drosophila* surface epithelia. Immunity *13*, 737–748.

Vail, P., Sutter, G., Jay, D., and Gough, D. (1971). Reciprocal infectivity of nuclear polyhedrosis viruses of the cabbage looper and alfalfa looper. J. Invertebr. Pathol. *17*, 383–388.

Vastag, L., Koyuncu, E., Grady, S.L., Shenk, T.E., and Rabinowitz, J.D. (2011). Divergent effects of human cytomegalovirus and herpes simplex virus-1 on cellular metabolism. PLoS Pathog. *7*, e1002124.

Wang, L.-L., Swevers, L., Rombouts, C., Meeus, I., Van Meulebroek, L., Vanhaecke, L., and Smagghe, G. (2019). A metabolomics approach to unravel cricket paralysis virus infection in silkworm Bm5 cells. Viruses *11*, 861.

Wang, L.-L., Swevers, L., Van Meulebroek, L., Meeus, I., Vanhaecke, L., and Smagghe, G. (2020). Metabolomic analysis of cricket paralysis virus infection in *Drosophila* S2 cells reveals divergent effects on central carbon metabolism as compared with silkworm Bm5 cells. Viruses *12*, 393.

Wu, P.C., Lin, Y.H., Wu, T.C., Lee, S.T., Wu, C.P., Chang, Y., and Wu, Y.L. (2018). MicroRNAs derived from the insect virus HzNV-1 promote lytic infection by suppressing histone methylation. Sci. Rep. *8*, 17817.

Xu, C., Franklin, B., Tang, H.-W., Regimbald-Dumas, Y., Hu, Y., Ramos, J., Bosch, J.A., Villalta, C., He, X., and Perrimon, N. (2020). An in vivo RNAi screen uncovers the role of AdoR signaling and adenosine deaminase in controlling intestinal stem cell activity. Proc. Natl. Acad. Sci. U S A *117*, 464–471. https://doi.org/10.1073/pnas.1900103117.

Yang, H., and Hultmark, D. (2017). *Drosophila* muscles regulate the immune response against wasp infection via carbohydrate metabolism. Sci. Rep. *7*, 1–14.

STAR★METHODS

KEY RESOURCES TABLE

REAGENT or RESOURCE	SOURCE	IDENTIFIER
Chemicals, peptides, and recombinant proteins		
40% sucrose water	Taiwan Sugar Corporation	Q-103794905-00052-8
Phosphate-buffered saline (PBS)	Protech Technology Enterprise Co., Ltd.	J373-4L
Trizol™ reagent	Thermo Fisher Scientific Inc.	CAT# 15596026
Chloroform	Sigma-Aldrich, Inc	C7559
Isopropanol	Echo Chemical Co., Ltd	CAT# 423830010
Ethanol	Sigma-Aldrich, Inc	V001229
RNase-free water	QIAGEN	CAT# 129112
Assay buffer	Cell Biolabs, Inc.	CAT# 268002
Enzyme mix	BioVision, Inc.	K413-100-3
Substrate mix	BioVision, Inc.	K413-100-4
PicoProbe	BioVision, Inc.	K413-100-2
Critical commercial assays		
Presto™ mini plasmid kit	Geneaid	PDH300
High capacity cDNA reverse transcription kit	Applied Biosystems	4368813
SensiFAST™ SYBR® Hi-ROX Kit	Bioline	BIO-92005
ATP determination kit	Molecular Probes, Inc.	P11496
Oligonucleotides		
siRNA-sl-gloverin, 5′-AGUCAGUCAAUCAGUCAGUCTT-3′	MDBio, Inc. (See STAR Methods)	N/A
siRNA-bm-gloverin-4, 5′-GCGUCUUGUUAGCUGCUUUTT-3′	MDBio, Inc. (See STAR Methods)	N/A
siRNA-control, 5′-UUCUCCGAACGUGUCACGUTT-3′	MDBio, Inc. (See STAR Methods)	N/A
Software and algorithms		
Prism 9.2	GraphPad	https://www.graphpad.com/scientific-software/prism/
NanoDrop 2000 spectrophotometer	Thermo Fisher Scientific	CAT# ND-2000
DNA Copy Number and Dilution Calculator	Thermo Fisher Scientific	https://www.thermofisher.com/tw/zt/home/brands/thermo-scientific/molecular-biology/molecular-biology-learning-center/molecular-biology-resource-library/thermo-scientific-web-tools/dna-copy-number-calculator.html
ABI StepOnePlus Real-Time PCR	Thermo Fisher Scientific	CAT# 4376600
FlexCycler^2 PCR thermal cycler	VWR International, LLC.	16055039
Epoch microplate spectrophotometer	BioTek Instruments, Inc.	N/A
SpectraMax Gemini EM microplate reader	Molecular Devices, LLC.	N/A

RESOURCE AVAILABILITY

Lead contact

Further information and requests for resources and reagents should be directed to and will be fulfilled by the lead contact, Yueh-Lung Wu (runwu@ntu.edu.tw).

Materials availability

This study did not generate new unique reagents.

Data and code availability

Additional information and data reported in this paper is available from the lead contact upon request.

EXPERIMENTAL MODEL AND SUBJECT DETAILS

Insects

Laboratory-cultured *S. litura* larvae were reared in cages kept in an environmental chamber at a constant temperature of 29 ± 1°C and under a 12:12 h light:dark cycle. Artificial feed to maintain the larvae was prepared according to the formula from a previous study (Koul et al., 1997). *B. mori* larvae of a tetra-molting hybrid [(Kou X Fu) X (Nung X Feng)] were supplied from the Miaoli District Agricultural Research and Extension Station, Taiwan. Larvae were reared on fresh mulberry leaves in a growth chamber at 26°C with a 16:8 light-dark photoperiod (Singh et al., 2013). Third- or fourth-instar larvae of *S. litura* and *B. mori* were collected depending on the experiment.

Cells and viruses

Cell lines SL1A and BmN derived from *S. litura* and *B. mori*, respectively, were cultured at 26°C in TC-100 insect medium (Gibco BRL) supplemented with 10% fetal bovine serum. Wild-type AcMNPV and BmNPV without any gene insertion and recombinant AcMNPV and BmNPV carrying the EGFP gene driven by *polyhedrin* promoter (Lin et al., 2020) were reproduced in SL1A and BmN cells, respectively, and the viral titers were measured by 50% tissue culture infectious dose ($TCID_{50}$) assay or real-time quantitative polymerase chain reaction (qPCR) (Chen et al., 2018; Lo and Chao, 2004). For the qPCR determination, we established standard curves for AcMNPV and BmNPV, respectively, using viruses with known titers of PFU/mL (determined in permissive cell lines) and their corresponding cycle threshold (Ct) values in qPCR, so the derived viral titers can be converted into $TCID_{50}$ titers in permissive cell lines.

METHOD DETAILS

Measurement of trehalose, glycogen, glucose, and adenosine in tissues

Third-instar larvae of *S. litura* and *B. mori* were individually injected with 1×10^6 PFU of AcMNPV or BmNPV. At 0, 24, and 48 hpi, the hemolymph and fat body were collected from the larvae. The concentration of trehalose, glycogen, glucose, adenosine in the hemolymph and fat body was determined by colorimetric methods using Trehalose Microplate Assay Kit (Cohesion Biosciences, Ltd., CAK1029), Glycogen Assay Kit (Cell Biolabs Inc., MET-5022), Glucose Assay Kit (Cell Biolabs Inc., STA-680), and Adenosine Assay Kit (Cell Biolabs Inc., MET-5090) respectively. Colorimetric methods using these commercially available kits have been established for insect samples in metabolic studies (Chang et al., 2020; Lin et al., 2020). For each measurement, we added necessary positive and negative controls for color development according to the manufacturers' manuals to ensure the effectiveness of colorimetric assays. Uninfected larval samples were included as negative control groups in each experiment to weigh the accurate changes in metabolites in experimental groups.

Analysis of gene expression by RT-qPCR

The hemolymph and fat body were collected from third-instar larvae at different time-points after the injection of 1×10^6 PFU of AcMNPV or BmNPV. For analyzing gene expression in cell lines, SL1A or BmN cells infected with one of the viruses at a multiplicity of infection (MOI) of 1 were collected. RNA was extracted from larval tissues or cells using TRIzol reagent (Invitrogen) according to a previously described procedure (Hu et al., 2018; Wu et al., 2018). Specifically, the tissue sample from two larvae or the cell sample (2×10^5) was lysed in 1 mL of TRIzol reagent. After homogenization by a pellet pestle, the sample was incubated at room temperature for 5 to 10 min. For fat body samples, the sample in TRIzol reagent was centrifuged for 10 min at 14,000 × g at 4°C and only the supernatant was collected. The sample in 1 mL TRIzol reagent was added with 0.2 mL chloroform and vigorously shaken for 15 sec. After incubation at room temperature for 10 min, the mixture was centrifuged at 14,000 × g for 15 min at 4°C. The upper aqueous phase was taken and added with 0.5 mL of isopropanol. After a 10-min incubation at room temperature, the mixture was centrifuged at 14,000 × g for 10 min. After decanting the supernatant, the pellet was washed with 1 mL of 75% ethanol by centrifugation at 7,500 × g for 5 min at 4°C. The RNA pellet was air-dried and dissolved in 50 μL of ddH_2O. The RNA concentration was quantified by a microvolume spectrophotometer (Thermo Scientific, Nanodrop 2000).

A PrimeScript™ RT reagent kit (Takara) was used to convert the RNA into cDNA as previously described (Chen et al., 2018). In brief, 2 μL of 5× PrimeScript™ buffer, 0.5 μL of RT enzyme mix, 0.5 μL of oligo dT

primers, and 0.5 μL of random hexamers were added to 500 ng of RNA in 6.5 μL of ddH_2O. The mixture was incubated at 37°C for 15 min for the reverse transcription reaction and then inactivated at 85°C for 5 sec. The obtained cDNA product was quantified using the spectrophotometer. To quantify the expression level of metabolic genes, specific primers were synthesized for qPCR. The reaction mixture comprised 10 μL of SYBR Green qPCR Master Mix (Bioline), 0.8 μL of primer (10 μM), 2 μL of cDNA, and 0.2 μL of sterilized water without RNase. The qPCR reaction was performed on an ABI PlusOne real-time system (Applied Biosystems, StepOnePlus™) with the following parameters: initiation at 95°C for 2 min, followed by 40 cycles of amplification at 95°C for 5 sec and at 60°C for 15 sec. Ct values were normalized by the $2^{-\Delta\Delta Ct}$ method. The relative expression level was calculated by dividing Ct of the target gene with that of the *18S* ribosomal RNA (rRNA) gene (Schmittgen and Livak, 2008). A list of primer sequences used in this study is given in Table S5.

ATP and ADP/ATP ratio analyses

To quantify the level of ATP in the samples, Molecular Probes® ATP Determination Kit (Invitrogen, A22066) was used as previously described (Chang et al., 2020; Lin et al., 2020). Specifically, fat bodies or hemolymphs from larvae, or SL1A and BmN cells infected by the virus, were lysed with cell culture lysis reagent that contained 25 mM Tris-phosphate (pH 7.8), 2 mM 1,2-diaminocyclohexane-N,N,N′,N′-tetraacetic acid, 2 mM DTT, 10% glycerol, and 1% Triton® X-100. Cell debris was removed by centrifugation at 14,000 rpm for 3 min, after which 10 μL of supernatant was transferred to the well of a 96-well black opaque plate containing 90 μL of the standard assay solution in each well. Standard ATP solutions, each of 10 μL, were added alongside on the same plate. After incubation at 28°C for 10 min, luminescence emitted at 560 nm was measured using a SpectraMax Gemini EM Microplate Reader (Molecular Devices). A standard curve was plotted using the relative light units (RLU) of the standard solution to calculate the ATP in the samples. To obtain the ADP/ATP ratio, we referred to a previous study (Song et al., 2017) in *Drosophila* and subjected supernatants after cell lysis to EnzyLight™ ADP/ATP Ratio Assay Kit (BioAssay Systems, ELDT-100). We followed the manufacturers' instructions for both ATP and ADP/ATP ratio analyses. Uninfected larvae or cells served as negative controls to ensure the validity of each measurement.

Phagocytosis assay

Fourth-instar larvae were each injected with 1×10^6 PFU of AcMNPV or BmNPV. Hemocytes were collected at 48 hpi, and then placed into the wells of a 96-well plate (4×10^4 cells/well). They were then mixed with FITC-labeled *E. coli* (4×10^4 cells/well) and the total volume supplemented by TC-100 culture medium to make a total of 100 μL per well. After culturing at room temperature for 60 min, cells were washed 2–3 times with 10% PBS and stained with 50 μL of 0.4% trypan blue for 10 min. After 2–3 washes with 10% PBS, the cells were fixed with 4% formaldehyde for 30 s. A counterstain was performed by adding 50 μL of DAPI (Thermo Fisher) for 30 min. After 2–3 washes with 10% PBS, cells were subjected to fluorescence microscopy. The phagocytotic activity of the hemocytes was assessed by quantifying the proportion of green fluorescence (from FITC-labeled *E. coli*) to blue fluorescence (from DPAI-stained hemocytes) (Bretscher et al., 2015).

Treatment of 2DG in cells and larvae

To determine the cytotoxicity of 2DG treatment, SL1A and BmN cells were seeded in 12-well plates (2×10^5 cells/well) and treated with 10, 20, and 50 mM of 2DG for 24, 48, and 72 h. The cytotoxicity was determined by an MTT [3-(4,5-dimethylthiazol-2-yl)-2,5-diphenyltetrazolium bromide] assay. At each time-point, the medium was removed and the cells were combined with 10 μL of the MTT solution (final concentration 0.5 mg/mL). After 1 h of incubation, the cells were placed into 96 well plates and absorption at 570 nm was measured using a microplate (ELISA) reader (BioTek). The survival rate (%) was calculated by dividing the absorbance by that of the cells without 2DG treatment.

To determine the effect in cells of 2DG treatment on virus infection, cells were pre-incubated with 10 mM of 2DG for 2 h prior to infection with AcMNPV or BmNPV (MOI of 1). To determine the effect in larvae, 5 μL of 10 mM 2DG was combined with 1×10^6 PFU AcMNPV or BmNPV and injected into *S. litura* or *B. mori* third-instar larvae. At 24 and 48 hpi, supernatants of cell cultures or larval tissues were harvested to determine the ATP levels, the expression of carbohydrate metabolic genes and gloverin genes, and the viral titer.

siRNA transfection

siRNAs of the gloverin and control were synthesized by MDBio, Inc., and had the following sequences: siRNA-sl-gloverin, 5′-AGUCAGUCAAUCAGUCAGUC-3′; siRNA-bm-gloverin-4, 5′-GCGUCUUGUUAG CUGCUUU-3′; siRNA-control, 5′-UUCUCCGAACGUGUCACGU-3′. All siRNA molecules were synthesized with 2-nt deoxythymidine (TT) 3′ overhangs as shown in Figure S7A. Double SL1A or BmN cells (2×10^5 cells/well) were seeded into 24-well plates and transfected with 100 pmol of siRNA-gloverin or siRNA-control using Lipofectamine RNAiMAX Reagent (Invitrogen). Total RNA of the transfected cells was extracted at 48 hpt. The transcript level of the target genes and a reference gene (*actin*) was confirmed by RT-PCR. To determine the permissiveness for viruses, at 24 hpt the transfected cells were infected with either AcMNPV or BmNPV at an MOI of 1. The cells were further incubated and supernatants harvested to detect viral titers and ATP levels at 48 hpi (Chen et al., 2018).

QUANTIFICATION AND STATISTIC ANALYSIS

For each experiment, at least three replicates were performed. GraphPad Prism 9.2 was used for statistical analysis and chart production. Student's *t*-test was used to evaluate significance between two groups, with significant differences marked by asterisks in the figures (*$p < 0.05$; **$p < 0.01$; ***$p < 0.005$). Comparisons of gene expression among three or more groups were analyzed by one-way ANOVA with Tukey's Honestly Significant Difference (HSD) *post-hoc* test, with significant differences indicated by asterisks in tables (*$p < 0.05$; **$p < 0.01$; ***$p < 0.005$). For plotting heat maps, logarithms of the standardized *Ct* values (Log_{10}) from RT-qPCR were calculated and the images were illustrated by Prism 9.2 (Hu et al., 2018).